



Macroscopic water vapor diffusion is not enhanced in snow

Kévin Fourteau¹, Florent Domine^{2,3}, and Pascal Hagenmuller¹

¹Univ. Grenoble Alpes, Université de Toulouse, Météo-France, CNRS, CNRM, Centre d'Études de la Neige, Grenoble, France

²Takuvik Joint International Laboratory, Université Laval (Canada) and CNRS-INSU (France), Québec, QC, G1V 0A6, Canada

³Centre d'Études Nordiques (CEN) and Department of Chemistry, Université Laval, Québec, QC, G1V 0A6, Canada

Correspondence: kfourteau@protonmail.com

Abstract. Water vapor transport in dry snowpacks plays a significant role for snow metamorphism and the mass and energy balance of snowpacks. The molecular diffusion of water vapor in the interstitial pores is usually considered as the main or only transport mechanism, and current detailed snow physics models therefore rely on the knowledge of the effective diffusion coefficient of water vapor in snow. Numerous previous studies have concluded that water vapor diffusion in snow is enhanced relative to that in air. Various field observations also indicate that for vapor transport in snow to be explained by diffusion alone, the effective diffusion coefficient should be larger than that in air. Here we show using theory and numerical simulations on idealized and measured snow microstructures that, although sublimation and condensation of water vapor onto snow crystal surfaces do enhance microscopic diffusion in the pore space, this effect is more than countered by the restriction of diffusion space due to ice. The interaction of water vapor with the ice results in water vapor diffusing more than inert molecules in snow, but still less than in free air, regardless of the value of the accommodation coefficient of water on ice. Our results imply that processes other than diffusion, probably convection, play a preponderant role in water vapor transport in dry snowpacks.

1 Introduction

When a snowpack is submitted to a temperature gradient, macroscopic water vapor transfer occurs from the warmer to the colder parts of the snowpack, in a process sometimes referred to as layer-to-layer vapor flux. This redistribution of mass plays a significant role in the evolution of the snowpack and its physical properties. In the absence of air convection in the snowpack, this macroscopic vapor flux results from the microscopic vapor diffusion occurring in the interstitial pores of snow, and is impacted by water sublimation and condensation processes acting as sources and sinks of vapor at the ice-pore interface (Yosida et al., 1955; Colbeck, 1983). While the physics at play in the pores is generally well understood (Pinzer et al., 2012; Calonne et al., 2014), the transition from the microscopic to the macroscopic scale remains a point of contention in the snow community (Giddings and LaChapelle, 1962; Colbeck, 1993; Sokratov and Maeno, 2000; Pinzer et al., 2012; Calonne et al., 2014). Yet, a proper understanding of vapor transport in snow at the macroscopic scale is a pre-requisite for accurate snowpack physical modeling.

There has been a long-standing controversy concerning the magnitude of the macroscopic diffusive fluxes transporting mass



from one layer to another, and in particular to determine whether they are larger than what would be observed in free air under
25 similar macroscopic vapor gradients. The pioneering study of Yosida et al. (1955) set out to measure in the laboratory the
macroscopic vapor flux in a pile of snow subjected to a thermal gradient. Their results indicated that contrary to first expect-
ations, the vapor flux was about 3 to 4 times larger than in free air. To explain this enhanced diffusion, Yosida et al. (1955)
introduced the "hand-to-hand" delivery mechanism, which notably considers that the condensation of water molecules on one
side of an ice grain and the sublimation on another side acts as a shortcut in the vapor trajectory. Several subsequent experi-
30 mental studies have either confirmed (e.g. Sommerfeld et al., 1987) or contradicted (Sokratov and Maeno, 2000) the findings
of Yosida et al. (1955) that macroscopic vapor diffusion is significantly larger in snowpacks than in free air. Similarly, several
analytical and numerical modeling works have either accepted (Colbeck, 1993; Christon et al., 1994; Gavriliiev, 2008; Hansen
and Foslien, 2015) or contradicted (Giddings and LaChapelle, 1962; Calonne et al., 2014) the results of Yosida et al. (1955) and
the hand-to-hand mechanism. As mentioned by Sokratov and Maeno (2000) and Pinzer et al. (2012) the experimental discrep-
35 ancies can be explained by the difficulty to accurately measure macroscopic vapor fluxes and vapor concentration gradients in
snow, either in the field or in the laboratory. Yet, the large disagreement between the various analytical and modeling works,
which sometimes differ more than tenfold (e.g., Colbeck, 1993; Calonne et al., 2014), cannot be explained by experimental
errors.

The aim of this paper is to clarify the origin of these discrepancies and to quantify the macroscopic vapor flux based on the-
40 oretical and numerical modeling. For this we first consider in Section 2 whether the hand-to-hand mechanism, as originally
proposed by Yosida et al. (1955), can indeed explain the large macroscopic vapor fluxes observed in snow. Then in Section 3,
we recall how the macroscopic vapor flux can be obtained from the microscopic vapor flux occurring at the pore scale. In
Section 4 we present theoretical work to quantify the macroscopic vapor flux in snow, with an emphasis on the impact of the
ice surface kinetics. Finally, numerical simulations are presented in Section 5 in order to illustrate the points raised throughout
45 the article and to provide some numerical values of the effective diffusion coefficient.

2 Does the hand-to-hand mechanism enhance macroscopic vapor diffusion?

As previously mentioned, the experiment of Yosida et al. (1955) marks the introduction of the idea of enhanced vapor diffusion
due to the hand-to-hand delivery mechanism. Their experimental set-up consisted of four stacked cans (3.5 cm in height and
5.5 cm in diameter each) filled with snow, and separated with wire meshes that held the snow in place in each can without
50 preventing vapor diffusion between them. A temperature difference was imposed between the top and bottom of the stack in
order to create a vertical thermal gradient of about 45 K m^{-1} , and thus induce a macroscopic vapor flux. The experiments were
carried out with average temperatures of about -4°C and lasted about 5 hours. The cans filled with snow were weighted be-
fore and after the experiment in order to determine their mass gain or loss, which can be used to estimate the magnitude of the
macroscopic vapor flux transporting mass from one can to another. Based on these measurements, and assuming that vapor was
55 at saturation concentration, Yosida et al. (1955) concluded that the macroscopic vapor flux was about 3 to 4 times greater than
what would be expected in free air for a similar concentration gradient. Noting that this result appears to contradict the idea



that the presence of ice would impede the diffusion of vapor in snow, Yosida et al. (1955) proposed the hand-to-hand delivery mechanism as an explanation for this contradiction. This mechanism first states that because of its low thermal conductivity, the pore phase of snow tends to concentrate the thermal gradient, leading to a concentrated vapor gradient in the pores. More-
60 over, Yosida et al. (1955) proposed that: "*Water vapor needs not force its way through the interspaces between the ice grains composing snow. It needs only condense on one side of an ice grain and evaporate from the other side to condense again on the side facing to it of the next grain. In this way the distance which the water vapor actually traverses by diffusion turns out to be a fraction of the distance of its displacement. Such a situation makes the diffusion of water vapor through snow easier*
65 *coefficient in free air*". One should note that this explanation entails more than the simple continuous sublimation of vapor from some interfaces and subsequent condensation on others. Yosida et al. (1955) argued that this is equivalent to a situation in which a molecule condensing on one side of an ice grain re-appears as a sublimating molecule on another side.

Our understanding is however that the second part of the mechanism proposed by Yosida et al. (1955) is not physically
70 sound, and that the continuous condensation and sublimation of molecules cannot be used to explain their experimental results. A schematic illustration of the experiment is given in Figure 1, with only two cans for simplicity. The hand-to-hand delivery of water molecules is represented by the orange and red dots, condensing on the lower side and sublimating on the upper side of the ice grain at the interface between the two cans. For this mechanism to explain the experimental observations, the continuous condensation and sublimation should produce a real mass flux from one can to the other, as if the condensing
75 molecule reappeared as the sublimating one. However, what actually happens is that the condensing molecule (represented as an orange dot in Figure 1) remains incorporated at the bottom of the ice grain, thus remaining in the first can. Similarly, the sublimating molecule (represented as a red dot in Figure 1) was already present in the second can. The synchronous sublimation and condensation therefore do not lead to a mass transfer between the two cans. This is different from the molecules traversing the boundary in the air phase (represented as green dots in Figure 1), that actually lead to a mass transfer by depleting the first
80 can in favor of the second one. We therefore argue that the hand-to-hand mechanism, as proposed by Yosida et al. (1955), is not physically sound.

One might be tempted to argue that the idea of water vapor shortcutting the ice phase is supported by the indistinguishability of water molecules. For an observer focused on the pore phase, the argument says, it really appears as if the water vapor is transported almost instantaneously through the ice phase, as a disappearing water molecule condensing on one side of an
85 ice grain is almost instantaneously replaced by an appearing molecule sublimating on the other side. However, this point of view neglects the fact that the mass leaving a control volume also depends on the gain or loss of the ice phase during the condensation/sublimation process. As exemplified in the right panel of Figure 1, for an observer focused on the ice phase everything appears as if the ice disappearing on the sublimation side reappeared on the condensing side (see for instance the videos in the Supplements of Pinzer et al., 2012; Hagenmuller et al., 2019). Because of mass conservation during the
90 sublimation/condensation process, the apparent flux of vapor skipping the ice phase is compensated by an equal counter-flux of water molecule in the ice phase. Therefore, the mass transfer from one control volume to another is solely governed by the

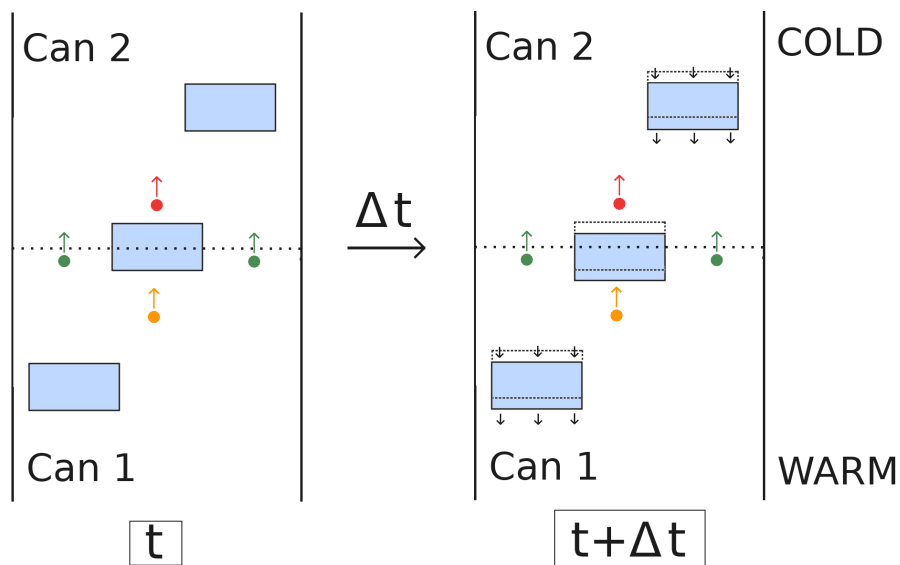


Figure 1. Illustration of the experiment of Yosida et al. (1955) (not to scale), with the ice phase represented in blue and the boundary between two cans represented as a dashed line. The green dots represent water molecule diffusing through the boundary between two cans. The orange and red dots are condensing and sublimating molecules, which are at the origin of the hand to hand mechanism as proposed by Yosida et al. (1955). The evolution of the system over a time period Δt is depicted in the right panel. The black arrows indicate the movement of the ice phase, opposite to that of water molecules in the gas phase.

diffusion of water molecules in the air phase (green dots in Figure 1).

We stress that we do not disagree with the insightful propositions of Yosida et al. (1955) (i) that the vapor flux tends to travel from one ice grain to another and not to go around them, and (ii) that the thermal gradient is enhanced in the pore space compared to the macroscopic gradient. The point of contention is that the continuous sublimation and condensation of water molecules does not count as a contribution to the mass flux. This problem with the hand-to-hand mechanism has been previously addressed by Giddings and LaChapelle (1962), when they noted that *"The hand-to-hand transfer does not contribute to the flux because this transfer does not shift water molecules across a plane fixed in the solid network"*.

The problem at hand is now to quantify the impact of the enhanced thermal gradient in the air phase on the macroscopic diffusion of vapor, and to determine whether it can account for the large macroscopic vapor fluxes reported in the literature (e.g. Yosida et al., 1955; Sommerfeld et al., 1987), and in particular if they can be superior to the fluxes in free air.

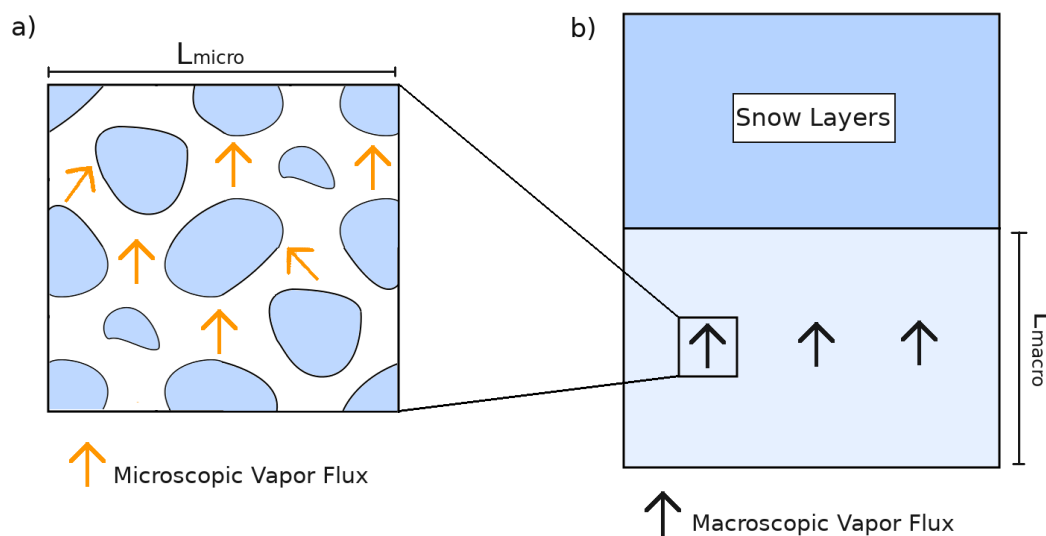


Figure 2. Relationship between the microscopic and macroscopic points of view of a snow sample. a) Microscopic point of view, with the ice phase in blue and microscopic vapor flux in orange. b) Macroscopic point of view where the snowpack is seen as a layered continuum.

3 Defining the macroscopic vapor flux and the effective diffusion coefficient

Let us consider a volume of snow (Figure 2a), submitted to vertical macroscopic temperature and vapor gradients at its boundaries. A necessary condition to be able to treat this snow sample as an equivalent macroscopic medium, is the condition of separation of scales (Auriault, 1991; Auriault et al., 2010). This separation of scale can be expressed as:

$$L_{\text{micro}} \ll L_{\text{macro}} \quad (1)$$

where L_{micro} is the length-scale characterizing the size of the Representative Elementary Volume (REV) (Auriault et al., 2010; Calonne et al., 2014) of the microstructure, and L_{macro} is the length-scale characterizing variations of the snowpack or solicitations at the macroscopic scale, for instance the change between different snow layers or changes in vapor gradient (Figure 2b). In this study we consider snow samples with a size of at least L_{micro} but less than L_{macro} . In this case, the snow sample is large enough to be treated as an equivalent macroscopic body, but no so large that it spans several snow layers and can thus be considered as macroscopically homogeneous. The relation between the various length-scales is exemplified in Figure 2.

At the microscopic scale, vapor diffuses in response to vapor concentration gradients in the pore space. The resulting microscopic vapor fluxes \mathbf{f} are governed by Fick's law: $\mathbf{f} = -D_0 \nabla c$, with D_0 being the diffusion coefficient of vapor in air and ∇c the gradient of vapor concentration in the pore. These microscopic fluxes may result in a net transport of mass at the macroscopic scale, i.e. a macroscopic flux. The magnitude of this macroscopic flux \mathbf{F} corresponds to the mass transported through an orthogonal plane per time unit and per unit surface of snow. This macroscopic flux is the quantity that Yosida et al. (1955)



set out to measure.

120 This paper, as previous works in the scientific literature, will determine the macroscopic flux from the first principles of physics
at the pore scale. It is therefore necessary to determine how the macroscopic flux \mathbf{F} at the macroscopic scale can be obtained
from the microscopic fluxes \mathbf{f} in the pores. One might attempt to compute \mathbf{F} as the quantity of matter transported through
an arbitrary plane of the microstructure. In this case, \mathbf{F} would be given as the surface average of the pore-scale flux \mathbf{f} , with
the averaging performed over the entire plane, ice phase included (the vapor flux being zero in the ice). Yet, this method of
125 computing the macroscopic vapor flux is problematic. Indeed, the macroscopic flux of the snow sample should be independent
of the choice of this arbitrary plane, otherwise the same snow sample could be assigned different macroscopic fluxes, con-
trary to the notion that the snow sample is homogeneous from the macroscopic point of view. The issue lies in the fact that
microscopic-scale variations of the vapor flux are not accessible at the macroscopic scale, where only slowly varying quanti-
ties are considered. The macroscopic flux should therefore be computed as the average microscopic vapor flux over the entire
130 representative volume of the microstructure. Again, the averaging needs to be performed over the total volume, including the
ice phase. Note that volume averaging is equivalent to averaging the vapor flux crossing multiple parallel planes spanning the
whole microstructure.

One can now phenomenologically define the effective diffusion coefficient for vapor D_{eff} such that $\mathbf{F} = -D_{\text{eff}}\nabla C$, where ∇C
is the macroscopic vapor concentration gradient. An intuitive definition of the macroscopic vapor gradient is the difference in
135 average vapor concentration between two opposing sides of the snow sample divided by the size of the sample. Here, the vapor
concentration is expressed in mass per volume of pore space, and the averaging is thus performed in the air phase only. This is
the definition implicitly adopted by Yosida et al. (1955). Ideally, the effective diffusion coefficient D_{eff} should be independent
of the applied thermal and vapor gradients. In this case, it is possible to treat the problem of macroscopic vapor transport in
snow with a generalized Fick's law, where D_{eff} is independent of the applied boundary conditions and only depends on the
140 snow microstructure. Such an effective diffusion coefficient does not depend on the external conditions, and is then said to be
intrinsic (Auriault et al., 2010). However, one should keep in mind that the effective diffusion coefficients computed in this
work might depend on the applied vapor and thermal gradients, and are therefore not necessarily intrinsic.

Finally, we define the normalized effective diffusion coefficient as $D_{\text{eff}}^{\text{norm}} = D_{\text{eff}}/D_0$. The normalized diffusion coefficient
allows us to easily compare the macroscopic vapor fluxes in snow and in free air.

145 4 Quantifying the macroscopic vapor flux in snow

Let us consider a snow sample of volume V submitted to vertical thermal and vapor concentration gradients. For simplicity,
we assume the problem to be steady-state. The diffusion of water vapor at the microscopic scale is governed by the following
system of equations (Calonne et al., 2014):

$$\begin{cases} \text{div}(-D_0\nabla c) = 0 & (\Omega_a) \\ -D_0\nabla c \cdot \mathbf{n} = \alpha v_{\text{kin}}(c - c_{\text{sat}}) & (\Gamma) \end{cases} \quad (2)$$



150 where Ω_a , Γ , and \mathbf{n} represent the pore phase, the ice/pore interface, and the normal vector to Γ pointing toward the ice. D_0 is the vapor diffusion coefficient in free air, c the vapor concentration in the pores, c_{sat} the vapor saturation concentration at the ice interface, $v_{\text{kin}} = \sqrt{(kT)/(2\pi m)}$ is related to the velocity of water molecules in the gas phase and is referred to as the kinetic velocity (k being Boltzmann's constant and m the mass of a water molecule), and α is the accommodation coefficient of water molecules on the ice surface, and is less than or equal to unity. The second equation of the system is the Hertz-Knudsen
155 equation and governs the mass fluxes that are incorporated or released from the ice phase. In the presence of a thermal gradient, the dependence of the saturation concentration to the local curvature of the ice surface can be neglected (Colbeck, 1983). Under this condition, c_{sat} becomes a function of temperature only.

The actual value of the α coefficient is not well-known, and in general will depend on the local saturation of water vapor and on the crystallographic properties of the ice surface (Saito, 1996; Libbrecht and Rickerby, 2013). Yet, two limiting cases,
160 corresponding to the case of infinitely fast surface kinetics and inert ice surfaces, can easily be analyzed. As will be empirically verified later, these two cases appear to correspond to the upper and lower bounds of macroscopic vapor fluxes in snow.

4.1 The infinitely fast surface kinetics case

In the case where the product αv_{kin} is very large, small oversaturations (or respectively undersaturations) lead to an abrupt ad-
sorption (respectively desorption) of water molecules, rapidly restoring the saturation value. In the limiting, and hypothetical,
165 case of infinitely fast surface kinetics (i.e. $\alpha v_{\text{kin}} \rightarrow \infty$), the vapor concentration is constantly at saturation at the ice/pore inter-
face. The Hertz-Knudsen equation can thus be replaced by the simpler equality of the vapor concentration with its saturation
value at the ice surface. This does not mean that the deposition and sublimation fluxes are zero at the interface.

As explained by Pinzer et al. (2012), it can be expected that the infinitely fast surface kinetics situation is the case where the
microscopic vapor gradients across the pores are maximal, and therefore where the macroscopic vapor flux is also maximal.
170 Note that the assumption of saturated vapor at the ice surface, and therefore infinitely fast surface kinetics, has been regularly
employed in studies about the diffusion of vapor in snow (e.g. Colbeck, 1993; Christon et al., 1994; Pinzer et al., 2012).

Even though this case appears to correspond to the maximal vapor flux, it can be shown that the macroscopic diffusion
coefficient remains inferior than expected in free air, as pointed out by Giddings and LaChapelle (1962). This is due to the loss
175 of diffusion space because of the ice phase, and we propose here to rederive the Giddings and LaChapelle (1962) demonstration,
using a more detailed framework. First, we assume that the thermal gradient is low enough, so that the saturation vapor
concentration dependence on temperature can be considered to be linear. For a thermal gradient of 100 K m^{-1} applied to a
1 cm sample, the deviation of vapor concentration from linear behavior is about 0.1%, while the deviation of the derivative
with respect to temperature is about 5%. Moreover, this condition corresponds to the fact that the macroscopic vapor gradient
180 should be constant over the sample, i.e. that the size of the sample is inferior to L_{macro} .



Under this assumption one can show that the vapor concentration is at saturation within the entire pore phase. A demonstration is presented in Appendix A, and a similar conclusion was also reached by Yosida et al. (1955) and Pinzer et al. (2012). Consequently, the macroscopic vapor flux is expressed as:

$$\mathbf{F} = \frac{1}{V} \int_V \mathbf{f} dV = \phi \frac{1}{V_a} \int_{V_a} -D_0 \nabla c_{\text{sat}} dV = \phi \frac{1}{V_a} \int_{V_a} -D_0 \frac{dc_{\text{sat}}}{dT} \nabla T_a dV \quad (3)$$

185 where ϕ is the snow porosity, V_a is the volume of the pore space, ∇T_a is the microscopic temperature gradient in the air, and where we have used the chain rule $\nabla c_{\text{sat}} = \frac{dc_{\text{sat}}}{dT} \nabla T_a$. As we considered that the saturation concentration of vapor does not deviate from a linear behavior, $\frac{dc_{\text{sat}}}{dT}$ is taken as constant over the volume V_a . Thus:

$$\mathbf{F} = -\phi D_0 \frac{dc_{\text{sat}}}{dT} \frac{1}{V_a} \int_{V_a} \nabla T_a dV \quad (4)$$

The precise relationship between the average microscopic thermal gradient in the air phase, and the macroscopic gradient
 190 ∇T depends on the particular snow microstructure (Calonne et al., 2011, 2014; Hansen and Foslien, 2015). However, Hansen and Foslien (2015) report that:

$$\nabla T = \phi \frac{1}{V_a} \int_{V_a} \nabla T_a dV + (1 - \phi) \frac{1}{V_i} \int_{V_i} \nabla T_i dV \quad (5)$$

where V_i is the volume of the ice phase and ∇T_i is the microscopic temperature gradient in the ice phase. As snow is a transversely isotropic material with the vertical direction being the direction normal to the isotropy plane, one can
 195 expect for reason of symmetry that the average air and ice thermal gradients are aligned with the vertical macroscopic gradient. Moreover, the average air and ice thermal gradients are oriented in the same direction as the macroscopic gradient. Therefore, one has the inequality about the magnitudes of the air and macroscopic thermal gradients:

$$\frac{1}{V_a} \left| \int_{V_a} \nabla T_a dV \right| \leq \frac{1}{\phi} |\nabla T| \quad (6)$$

which states that while the average thermal gradient in the air can be superior to the macroscopic thermal gradient, it
 200 cannot exceed it by a more than $1/\phi$ factor. Intuitively, it states that the temperature drop in the pore phase cannot exceed the temperature drop observed over the entire snow sample. One can show that the air thermal gradient is maximal in the special case of a microstructure composed of slabs perpendicular to the macroscopic temperature gradient. In this case the temperature gradient is almost entirely concentrated in the air, and furthermore Equation 6 becomes an equality when the



thermal conductivity of ice is assumed to be infinite.

205 Using the inequality of Equation 6 in Equation 4, leads to an inequality on the magnitude of the macroscopic flux:

$$|\mathbf{F}| \leq D_0 \frac{dc_{\text{sat}}}{dT} |\nabla T| = D_0 |\nabla C| \quad (7)$$

where $\nabla C = \frac{dc_{\text{sat}}}{dT} \nabla T$ is the macroscopic vapor concentration gradient.

The macroscopic vapor flux is thus inferior to the vapor flux that would take place in free air, which can be similarly
210 expressed by $D_{\text{eff}}^{\text{norm}} \leq 1$. While the microscopic vapor flux in the pore phase is enhanced due to the enhancement of the
microscopic temperature and vapor gradients, this effect is countered by the reduction of the space where vapor can diffuse.
As the average air temperature gradient is at the maximum enhanced by a factor $1/\phi$ while the reduction of pore space
systematically decrease the macroscopic flux by a factor ϕ , the resulting macroscopic vapor flux cannot be greater than in free
air. The equality $D_{\text{eff}}^{\text{norm}} = 1$ holds when the entire temperature gradient is concentrated in the pore phase. However, since the
215 thermal conductivity of ice is finite, the thermal gradient cannot be solely concentrated in the pore phase and thus one always
has $D_{\text{eff}}^{\text{norm}} < 1$.

4.2 The slow surface kinetics case

The other limiting case is when the condensation and sublimation of water vapor at the ice grain surfaces is slow enough to be
neglected. The diffusion of water vapor in snow then becomes equivalent to the diffusion of a gas in an inert porous structure.
220 This problem has been extensively studied (e.g. Torquato and Haslach Jr, 2002; Auriault et al., 2010), and in this case the
effective diffusion coefficient is given by:

$$D_{\text{eff}} = \phi \tau D_0 \quad (8)$$

where τ is defined as the tortuosity factor and is linked to the lengthening of the diffusion streamlines in the porous network.
The tortuosity factor represents an impediment of diffusion, and is thus inferior or equal to unity. Moreover, τ depends solely
225 on the structure of the porous medium and not on the specific diffusive specie or the applied concentration gradient (Torquato
and Haslach Jr, 2002; Auriault et al., 2010). Under an assumption of slow surface kinetics, Calonne et al. (2014) report effective
diffusion coefficients reduced from 20 to 85% compared to the free air case, with lower diffusion coefficients corresponding to
denser snow samples. Although we do not have a rigorous demonstration of this fact, it appears that the slow kinetics assump-
tion corresponds to the case where the macroscopic flux (and hence D_{eff}) is minimal for a given vapor concentration gradient.
230 This proposition will be empirically verified with numerical simulations in Section 5.



4.3 Comparison with previous works

We have established in Section 4.1 that even under the assumption of fast surface kinetics, the effective vapor diffusion coefficient in snow cannot be superior to that in free air. Yet several studies based on analytical and numerical models, which are not subjected to experimental errors, have reported opposite results. It thus appears important to elucidate why those previous results do not invalidate the demonstration made in Section 4.1 and the results of this work.

Colbeck (1993) proposed a theoretical model, based on an idealized structure of disconnected and equally spaced ice spheres. In that model the vapor concentration is at saturation at the ice surface (i.e. surface kinetics are infinitely fast) and the vapor flux between two consecutive spheres can be analytically computed. In this case, the author concludes that the vapor diffusion coefficient is between four to seven times greater than in air. However, as pointed out by Pinzer et al. (2012), Colbeck (1993) derives the diffusion coefficient in snow by computing the flux crossing a single plane between two spheres, and not by averaging over the entire volume. As the plane between two spheres corresponds to a zone of maximal thermal gradient without any ice blockage, it is not surprising that the local microscopic vapor flux is several-fold that in free air. However, as will be seen in Section 5.1, computing the macroscopic flux by performing a volume averaging of microscopic vapor fluxes over the entire microstructure significantly reduces the corresponding diffusion coefficient, down to a value below that of free air.

Christon et al. (1994) performed one of the first finite element microscale simulations of vapor diffusion in snow under a thermal gradient, using an idealized microstructure. They concluded that the vapor diffusion coefficient is between one and two times as large as that in air. Yet, in that study the macroscopic mass flux is not computed as a volume average, but rather *"as the weighted average of the mass flux rates over all of the exterior surfaces of the diffusion domain in order to capture the bulk vertical mass diffusion rate"*. Here, the diffusion domain refers to the domain where vapor diffusion occurs, i.e. the pore space. This differs from volume averaging and leads to an overestimation of the macroscopic flux, as the ice phase is not included. As the loss of diffusion space due to the ice phase is neglected, the effective diffusion coefficient is overestimated by a $1/\phi$ factor. Similarly, Pinzer et al. (2012) performed finite element microscale simulations of vapor diffusion, this time with microstructures measured by tomography scanning. A diffusion coefficient slightly superior to that in free air is reported. Pinzer et al. (2012) noted that computing the mass flux crossing a single plane was insufficient, for the reasons discussed in Section 3. To derive the macroscopic mass flux, Pinzer et al. (2012) computed the average mass flux in each plane, and then averaged over all planes. However, it appears from the description of their methodology that the slice averaging was only performed in the pore phase, not taking into account the reduction of macroscopic flux due to the presence of ice. As in the case of Christon et al. (1994), this would explain the diffusion coefficient higher than in free air. As will be shown in Section 5, performing similar numerical simulations and computing the macroscale flux by total volume averaging leads to diffusion coefficients below that in free air.

Finally, Hansen and Foslien (2015) proposed an analytical expression for the effective thermal conductivity of snow, taking into account the latent heat associated with the transport of water vapor. One application of this effective thermal conductivity model is to allow the derivation of the vapor flux, which leads to the conclusion that the macroscopic vapor flux is superior to



that in free air. To come to this conclusion, Hansen and Foslien (2015) determine the vapor flux by identifying the contribution of latent heat in their expression of the effective thermal conductivity. However, during the identification of the latent heat contribution to the total energy flux, some of the heat conduction contribution of the ice phase is attributed to the latent heat transport. This leads to an artificially increased vapor flux, and therefore an overestimated diffusion coefficient. A re-derivation of the vapor flux with the thermal conductivity expression proposed by Hansen and Foslien (2015) is presented in Appendix B and leads to a macroscopic vapor flux below that in free air.

Most of the discrepancies between our results and those of the published literature thus reduce down to computations of the macroscopic fluxes that are inconsistent with fluxes expressed per unit surface of snow, as used in snow models and experimental studies. This leads to an overestimation of the value of the effective diffusion coefficient. Focusing on the magnitude of microscopic vapor fluxes as done by Colbeck (1993) or Christon et al. (1994) is of a great interest for snow metamorphism, as they govern the mass transfer between adjacent ice grains and the recrystallization rate. However, they do not correspond to the macroscopic mass flux expressed per unit surface of snow, as measured by Yosida et al. (1955) and subsequent experimental studies (e.g. Sokratov and Maeno, 2000). We reiterate that the macroscopic vapor flux responsible for the redistribution of mass at the macroscopic scale, and which inspired the hand-to-hand delivery mechanism, corresponds to the volume-averaged flux over the entire snow microstructure and must include the loss of diffusion space due to the ice phase.

5 Numerical modeling

In this section we present steady-state 3D numerical simulations of vapor diffusion in snow subjected to a macroscopic temperature gradient ∇T and a macroscopic vapor gradient ∇C . The macroscopic temperature gradient ∇T is obtained by imposing the top and bottom temperatures T^{top} and T^{bot} . The vapor concentrations in the pore space at the top and bottom of the sample are imposed to correspond to the saturation values for the top and bottom temperatures. We thus have:

$$|\nabla C| = \frac{|c_{\text{sat}}(T^{\text{top}}) - c_{\text{sat}}(T^{\text{bot}})|}{L_z} \quad (9)$$

where L_z is the height of the sample considered. Conditions of zero heat and vapor normal fluxes are imposed on the other sides of the sample. For simplicity, we only consider the case of vertical temperature and vapor gradients, although the extension to the other directions is straight forward. Moreover, we do not take into account the impact of latent heat on the temperature field. Taking it into account would reduce the air temperature gradient and would not increase the effective vapor diffusion coefficient.

The thermal conductivities of the ice and pore phases are set to 2.34 and 0.024 W K⁻¹ m⁻¹ respectively, and the diffusion coefficient of vapor in air D_0 is set to 2×10^{-5} m² s⁻¹. The vapor concentration is assumed to follow the Clausius-Clapeyron and ideal gas laws, leading to

$$c_{\text{sat}} = \frac{M}{RT} P_0 e^{\left(\frac{\Delta H_s}{R} \left(\frac{1}{T_0} - \frac{1}{T}\right)\right)} \quad (10)$$



where $M = 18 \times 10^{-3} \text{ kg mol}^{-1}$ is the molar mass of water, $R = 8.314 \text{ J K}^{-1} \text{ mol}^{-1}$ is the ideal gas constant, $\Delta H_s = 51 \times 10^3 \text{ J mol}^{-1}$ is the latent heat of sublimation of ice, $T_0 = 273.15 \text{ K}$ is a reference temperature, and $P_0 = 611 \text{ Pa}$ is the saturation pressure of vapor over ice at T_0 . All simulations are performed with an average temperature $(T^{\text{bot}} + T^{\text{top}})/2 = 258 \text{ K}$.

300 The heat and diffusion equations are solved using the finite element method with the open-source software Elmer (Malinen and Råback, 2013). In particular we use the readily available Elmer modules dedicated to the heat and diffusion equations, which are solved with iterative methods. The outputs of the simulations are then processed using the ParaView software.

As seen previously, the kinetics of the sublimation and condensation processes at the ice surface might significantly impact
305 the magnitude of the macroscopic vapor flux. We recall that in general the boundary condition at the ice/air interface is given by the Hertz-Knudsen equation:

$$-D_0 \nabla c \cdot \mathbf{n} = \alpha v_{\text{kin}}(c - c_{\text{sat}}) \quad (11)$$

where $v_{\text{kin}} \simeq 140 \text{ m s}^{-1}$ at 258 K , and α is the accommodation coefficient less than or equal to unity. In general α is not a constant and depends on the local vapor saturation as well as the crystallographic properties of the underlying ice crystal
310 (Saito, 1996; Libbrecht and Rickerby, 2013).

For each microstructure, several simulations were performed with different values of α in order to assess the impact of the internal boundary conditions (IBC) applied at the ice surface. We first performed simulations with constant α equal to $0, 10^{-5}, 10^{-4}, 10^{-3}, 10^{-2}, 10^{-1}$, and 1 . Simulations with constant α are referred to as linear kinetics simulations in what follow. Among them, a special case is $\alpha = 0$ which corresponds to the diffusion of vapor in an inert porous medium. Moreover, we
315 performed simulations similar to those of Christon et al. (1994) and Pinzer et al. (2012) where the Hertz-Knudsen boundary condition is replaced with the saturation of vapor at the ice surface. Finally, we performed simulations in which the dependence of α to the local vapor saturation is explicitly represented. For that we set $\alpha = \exp(-\sigma_0/\sigma)$ where $\sigma = (c - c_{\text{sat}})/c_{\text{sat}}$ and $\sigma_0 = 0.01$. Note that this expression was determined for the attachment of vapor to the basal and prismatic facets of ice crystals (Libbrecht and Rickerby, 2013), and might not properly apply for ice in snowpacks. However, this expression is useful
320 to study the potential impact of the dependence of α to the local vapor saturation. This type of simulation is referred to as non-linear kinetics simulations. Finally, the macroscopic fluxes of the various simulations are computed by performing a total volume average, as defined in Section 3, and the effective diffusion coefficients are obtained by dividing these macroscopic fluxes by the macroscopic concentration gradients, i.e. $D_{\text{eff}} = -\mathbf{F}/\nabla C$.

325 5.1 Idealized structure

We start with an idealized microstructure composed of disconnected ice spheres, similar to that used by Colbeck (1993). The structure is visible in Figure 3. The domain is a cuboid of dimension $3.7 \times 3.7 \times 10 \text{ mm}^3$, with three equidistant ice spheres with 3 mm diameters and which are vertically aligned at the center of the domain. The distance between two sphere centers is set to

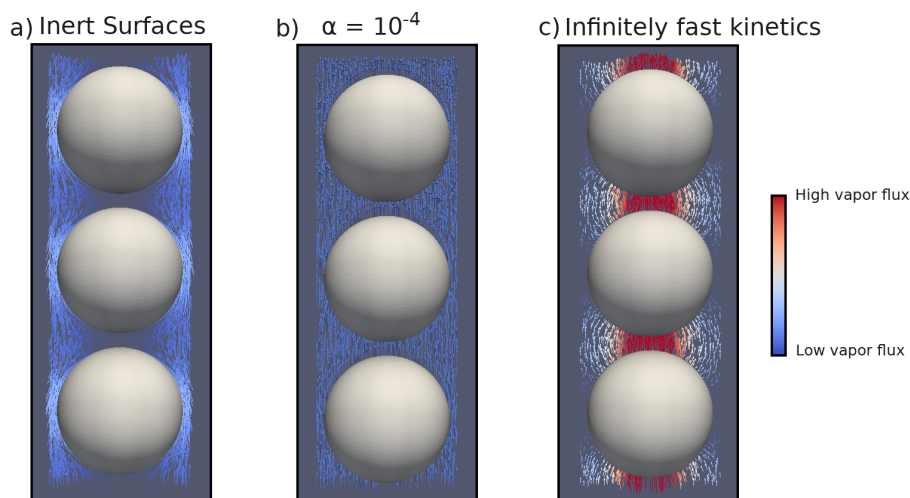


Figure 3. Disconnected ice spheres geometry with microscopic vapor fluxes in the pore space and for a 50 K m^{-1} thermal gradient. a) Inert surfaces case, b) $\alpha = 10^{-4}$ case, and c) infinitely fast kinetics case.

3.3 mm. This microstructure is characterized by a porosity of 0.619 and a density of 349 kg m^{-3} .

330 The simulations were performed for the different IBCs described previously and for temperature gradients ranging from 5 to 200 K m^{-1} . The resulting normalized effective diffusion coefficients are displayed in Figure 4.

We first analyze the 50 K m^{-1} temperature gradient simulations. Illustrations of the microscopic vapor fluxes for three IBCs, namely inert surfaces ($\alpha = 0$), $\alpha = 10^{-4}$ and infinitely fast surface kinetics, are displayed in Figure 3. In the case of inert
335 surfaces the vapor flux needs to go around the ice grains, which act as blockage, leading to tortuous stream lines. In the case of infinitely fast surface kinetics, the vapor flux does not need to go around the ice grain and is rather moving from ice grain to ice grain, in agreement with the suggestion of Yosida et al. (1955) and the numerical simulations of Pinzer et al. (2012). Finally, the $\alpha = 10^{-4}$ case displays an intermediate behavior, with some of the vapor flux moving from ice grain to ice grain, while the rest bypasses the ice phase. This exemplifies that the microscopic vapor fluxes are strongly dependent on the kinetics
340 of the vapor sublimation and deposition at the ice surface.

In the case of infinitely fast surface kinetics we find a normalized diffusion coefficient of 0.978, i.e. lower than in air, in agreement with the calculations of Section 4.1. Moreover, we computed the average air temperature gradient (in the pore phase only), and found it to be 77.57 K m^{-1} . This is enhanced compared to the 50 K m^{-1} macroscopic gradient, but still respects the inequality of Equation 6. While the enhancement of the thermal gradient increases the microscopic vapor fluxes in the pores,
345 it does not suffice to counter the loss of diffusion space, and the resulting macroscopic flux is lower than in free air.

To compare our results to the works of Colbeck (1993), Christon et al. (1994), and Pinzer et al. (2012), who worked under the similar assumption of infinitely fast kinetics, we used two alternate methods, different from total volume averaging, to compute the vapor flux. The first consists in averaging the microscopic vapor fluxes in the air phase only, and we call the associated



normalized diffusion coefficient $D_{\text{air}}^{\text{norm}}$. The second one consists in computing the flux crossing an horizontal plane placed
350 between two spheres, and we call the associated diffusion coefficient $D_{\text{plane}}^{\text{norm}}$. As explained in Section 4.3, we believe that the
first methodology is akin to works of Christon et al. (1994) and Pinzer et al. (2012), while the second was used by Colbeck
(1993). Calculations yield a $D_{\text{air}}^{\text{norm}}$ of 1.580 and a $D_{\text{plane}}^{\text{norm}}$ of 2.986, consistent with the values reported by Christon et al. (1994),
Pinzer et al. (2012), and Colbeck (1993). By not including the ice phase in the averaging or by selecting a peculiar plane where
microscopic vapor fluxes are maximum, the macroscopic vapor flux is overestimated, leading to a diffusion coefficient greater
355 than D_0 .

The outcome of the other simulations performed with $\nabla T = 50 \text{ K m}^{-1}$ is reported in Figure 4 and indicates that $D_{\text{eff}}^{\text{norm}}$ is
maximal in the infinitely fast kinetics case, with a value of 0.978, and minimal in the inert surfaces case, with a value of 0.512.
Accordingly, the normalized effective diffusion coefficient increases with α , and for the cases $\alpha = 0.1$ and $\alpha = 1$ differs by less
than 0.3% from the infinitely fast case. The use of the non-linear surface kinetics law leads to a normalized effective diffusion
360 coefficient equals to 0.857, in between the inert ($D_{\text{eff}}^{\text{norm}} = 0.512$) and infinitely fast kinetics ($D_{\text{eff}}^{\text{norm}} = 0.978$) cases.

Similar observations can be made for the simulations performed with other temperature gradients. For the entire range
of gradients tested, the infinitely fast kinetics and inert surfaces cases correspond to the maximal and minimal macroscopic
fluxes. Moreover, the associated effective diffusion coefficients are mostly independent of the macroscopic thermal or vapor
365 gradients, suggesting that the effective diffusion coefficients could be intrinsic in these cases. Consistent results are observed
for the simulations where α is constant. The obtained effective diffusion coefficients are mostly independent of the applied
macroscopic gradient, and are bounded by the infinitely fast kinetics and inert surfaces cases. Note that the $\alpha = 0.1$ and $\alpha = 1$
cases are indistinguishable from the infinitely fast kinetics results in Figure 4. Contrary to the rest of the simulations, the
non-linear IBC yields effective diffusion coefficients that depend on the magnitude of the applied gradients. In this case, the
370 macroscopic vapor flux and the macroscopic vapor concentration gradient are not proportionally linked by a single and well-
defined material property. Furthermore, for low vapor and thermal gradients the non-linear case is close to the inert surfaces
case while a transition towards the fast kinetics case is observed for thermal gradients around 50 K m^{-1} . Again, even though
the non-linear law used to express α as a function of local saturation does not necessarily accurately model water molecule
attachment in real snow, it illustrates the effects of a non-constant α .

375 5.2 Measured snow microstructures

Other numerical simulations of vapor diffusion have been performed, this time using measured snow microstructures instead
of the idealized structure of Section 5.1. The microstructures were obtained by X-ray tomography scanning of snow samples.
In total 6 snow samples were analyzed, covering the snow types of decomposing and fragmented precipitation particles (DF),
depth hoar (DH), rounded grains (RG), and melt forms (MF) (Fierz et al., 2009). The goal is not to provide effective diffusion
380 coefficients on an exhaustive set of snow microstructural patterns but to illustrate the effects of the snow microstructure and
surface kinetics on water vapor diffusion.

A zoom showing the vapor stream lines inside the melt forms sample is provided in Figure 5. As with the idealized microstruc-

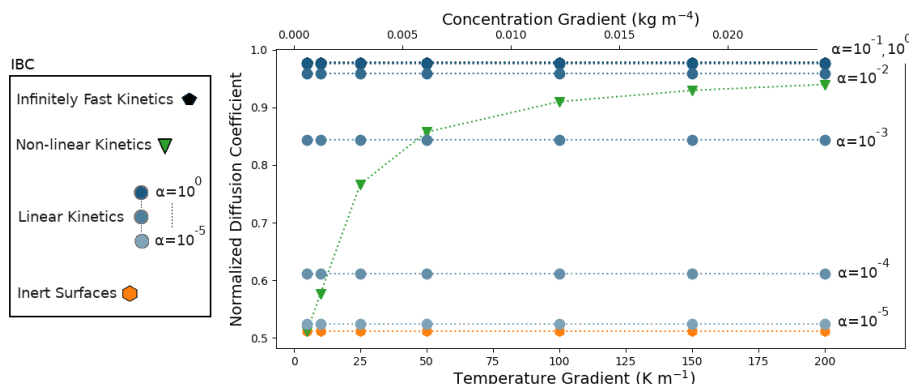


Figure 4. Normalized diffusion coefficients $D_{\text{eff}}^{\text{norm}}$ in the idealized spheres microstructure, for different temperature/vapor gradients, different IBCs and a mean temperature of 258 K. Note that the $\alpha = 0.1$, $\alpha = 1$, and infinitely fast kinetics cases are indistinguishable at the top of the graph.

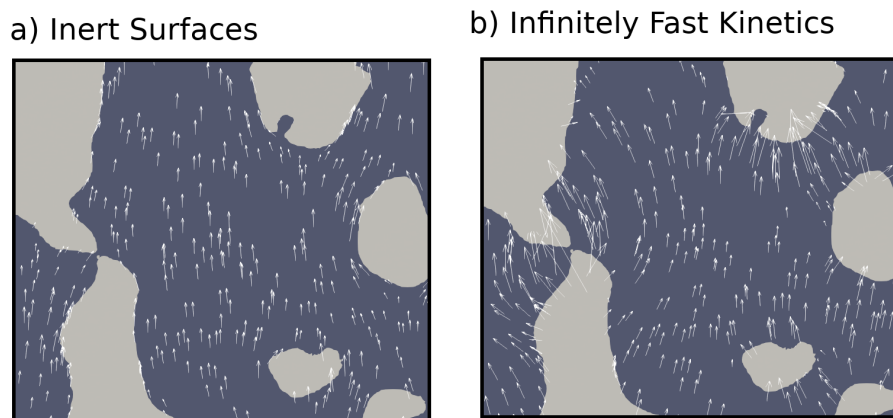


Figure 5. Vapor streamlines inside the melt forms sample, for a temperature gradient of 50 K m^{-1} and the inert surfaces and infinitely fast kinetics cases. Note that the arrows showing the vapor flux are centered around the point they represent, and might therefore wrongly appear to originate from or terminate in the ice phase.

ture, in the inert surface case vapor tends to go around the ice grains. In the infinitely fast kinetics case, vapor moves from ice grain to ice grain, as proposed by Yosida et al. (1955) and reported by Pinzer et al. (2012).

385

We start by analyzing the results of the simulations of the DF sample, characterized a density of 125 kg m^{-3} . Similarly to Section 5.1, the simulations were performed by imposing external temperature and vapor gradients, with different selected IBCs characterizing the kinetics of the vapor sublimation and deposition process. The results are displayed in Figure 6. As in the idealized case, the inert surface, infinitely fast kinetics, and linear kinetics cases yield normalized effective diffusion coef-

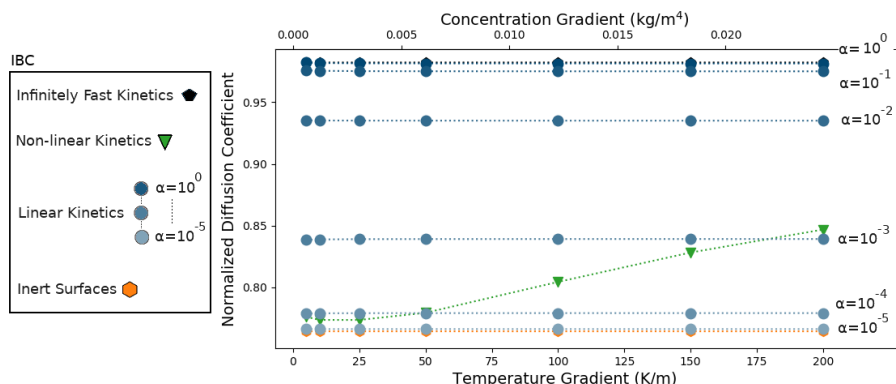


Figure 6. Normalized diffusion coefficients $D_{\text{eff}}^{\text{norm}}$ with a DF snow microstructure, for different temperature/vapor gradients, different IBCs and a mean temperature of 258 K. Note that the $\alpha = 1$ and the infinitely fast kinetics cases are superimposed at the top of the graph, and that the $\alpha = 10^{-5}$ and the inert surface cases are indistinguishable at the bottom of the graph.

390 ficients that are mostly independent of the applied gradients. Moreover, we observe that $D_{\text{eff}}^{\text{norm}}$ is minimal in the inert surface
 case with a value of 0.764, and maximal in the infinitely fast kinetics case with a value of 0.982. As expected, the effective
 diffusion coefficient is systematically lower than that of air. The normalized effective diffusion coefficients in the linear kinetics
 cases are distributed between the inert and infinitely fast values, and increase with the value of α . For $\alpha = 1$, $D_{\text{eff}}^{\text{norm}}$ differs by
 less than 0.1% from the infinitely fast kinetics case.

395 On the contrary, the non-linear kinetics case leads to a normalized effective diffusion coefficient that depends on the external
 gradients. As with the idealized disconnected spheres structure of Section 5.1, we observe that for low gradients the non-linear
 case is close to the slow kinetics simulations, and transitions towards faster kinetics with higher gradients. However, in the case
 of the DF sample this transition occurs more slowly and with higher temperature and vapor gradients.

400 Since the normalized effective diffusion coefficients appear to be independent of the external thermal/vapor gradient in the
 case of infinitely fast and linear surface kinetics, we only computed $D_{\text{eff}}^{\text{norm}}$ with a 50 K m^{-1} gradient for the 5 remaining
 snow samples. Moreover, we did not compute $D_{\text{eff}}^{\text{norm}}$ with non-linear surface kinetics (i.e. when alpha is not constant). The
 resulting $D_{\text{eff}}^{\text{norm}}$ values are reported in Table 1, and displayed in Figure 7 as a function of the snow density. Again, $D_{\text{eff}}^{\text{norm}}$
 is systematically minimal in the inert surface case and maximal in the infinitely fast kinetics. Consistently, the normalized
 405 effective diffusion coefficient increases with α . Furthermore, we observe an almost systematic decrease of $D_{\text{eff}}^{\text{norm}}$ with density.

6 Discussion

We have shown that the macroscopic vapor flux in snow cannot be larger than the flux in free air under the same water vapor
 gradient. This result is supported by a formal demonstration, inspired by the work of Giddings and LaChapelle (1962), as well
 as by numerical simulations on idealized and measured snow microstructures. While the interaction of water vapor with the



Table 1. Normalized effective diffusion coefficient for the 6 samples studied in the article, and as a function of surface kinetics. Values are derived from simulations with a 50 K m^{-1} thermal gradient, but our results suggest that they are independent of the thermal gradient. Snow types are classified according to Fierz et al. (2009) and SSA stands for Specific Surface Area.

Snow Type	Density (kg m^{-3})	SSA ($\text{m}^2 \text{ kg}^{-1}$)	Inf. Fast Kinetics	$\alpha = 1$	$\alpha = 10^{-1}$	$\alpha = 10^{-2}$	$\alpha = 10^{-3}$	$\alpha = 10^{-4}$	$\alpha = 10^{-5}$	$\alpha = 0$
				DF	125	40	0.982	0.981	0.975	0.935
DH	145	29	0.982	0.982	0.977	0.943	0.841	0.763	0.744	0.741
DH	156	26	0.977	0.977	0.973	0.942	0.840	0.744	0.718	0.714
DH	177	18	0.963	0.963	0.960	0.937	0.845	0.723	0.674	0.665
RG	316	34	0.913	0.910	0.894	0.807	0.646	0.561	0.539	0.532
MF	380	5	0.531	0.531	0.530	0.519	0.460	0.359	0.311	0.299

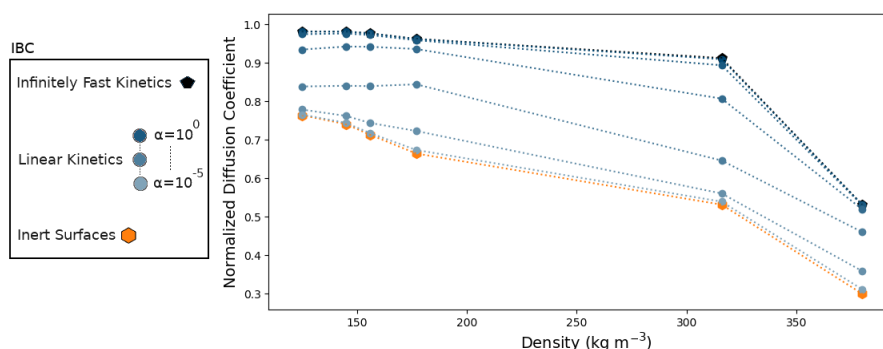


Figure 7. Normalized diffusion coefficients $D_{\text{eff}}^{\text{norm}}$ as a function of density, for the 6 snow samples considered in this paper.

410 ice structure results in a macroscopic flux larger than that of the inert diffusion case, the macroscopic vapor flux cannot be enhanced compared to the free air case.

As seen in this work, the sublimation/condensation fluxes at the ice surface play a great role on the final macroscopic flux. In particular we have shown that when the reaction is fast, i.e. α is large, the macroscopic fluxes can be close to those that would be observed in free air. Moreover, the dependence of α on the local vapor saturation might break the proportionality between
 415 the macroscopic vapor gradient and the macroscopic flux. In this case, it is no longer possible to define a single effective diffusion coefficient D_{eff} that proportionally relates the vapor flux to vapor gradient, and that solely depends on the snow microstructure. In other words, with non-linear surface kinetics D_{eff} is not intrinsic. For all these reasons, it appears important to determine what are the precise internal boundary conditions that govern the sublimation and condensation of water vapor in



snowpacks, and in particular to determine whether the inert surfaces or infinitely fast kinetics case could accurately describe
420 real snow. In the case of fast kinetics, one can have $D_{\text{eff}} \geq \phi D_0$, as the average microscopic vapor gradient can be greater than
the macroscopic vapor gradient. On the contrary, in the case of slow surface kinetics one has $D_{\text{eff}} = \phi \tau D_0 \leq \phi D_0$, since $\tau \leq 1$.
An experimental distinction between fast and slow kinetics could thus be made by observing whether the quantity $D_{\text{eff}}/(\phi D_0)$
is superior to unity or not. Using the experimental results of Sokratov and Maeno (2000), which are the experimental results
with the lowest reported diffusion coefficient, we observe that $D_{\text{eff}}/(\phi D_0)$ is almost always superior to unity, which supports
425 the notion of fast rather than slow kinetics. That being said, experimental determination of the macroscopic vapor fluxes is
difficult, as exemplified by the large spread of reported values, and more observations would be needed to decisively conclude
on this point.

This work investigated the effective diffusion coefficient of vapor in snow with a phenomenological approach, where the
diffusion coefficient is simply defined as the ratio of the macroscopic vapor flux to the vapor concentration gradient. A rigorous
430 upscaling of the microscale equations to derive the equivalent macroscopic formulation would greatly benefit the understanding
and modeling of the macroscopic vapor flux. Note that such an approach was used by Calonne et al. (2014) with the method
of asymptotic-scale expansion, but limited itself to small α . Applying a similar method to the case of non-negligible surface
sublimation and condensation would lead to a proper definition of the macroscopic quantities, notably of the effective diffusion
coefficient, and to the proper formulation of the equations governing the macroscopic scale.

435 Finally, the fact that there is no macroscopic enhancement of the water vapor flux in snow suggests that most of the mass flux
observed in subarctic and Arctic snow, and which would necessitate effective diffusion coefficients several times higher than
that of free air to be explained solely by diffusion (e.g. Domine et al., 2016, 2018), could rather be due to convection. The
importance of convective mass transport in subarctic snowpack has notably been pointed out by Trabant and Benson (1972)
and Sturm and Johnson (1991). Currently, detailed snow physics models do not include the mechanism of convective mass
440 transport (Lehning et al., 2002; Vionnet et al., 2012) and assume all mass transport to result from diffusion, sometimes using a
diffusion coefficient much larger than that in free air. Further modeling efforts to include convective mass transport in detailed
snow models could enhance their ability to model snowpack evolution.

7 Conclusions

This work investigated the macroscopic vapor fluxes that arise in snowpacks due to large scale vapor gradients. We first
445 considered the seminal work of Yosida et al. (1955) and their formulation of the hand-to-hand delivery mechanism, which
was meant to explain the large vapor flux they measured. We argue that it is reasonable to assume that the concentration of
the thermal gradient in the pore phase would lead to strong vapor gradients between ice grains, and drive the sublimation of
water molecules from some grains and subsequent condensation on others. Yet, we disagree with the proposed idea that the
process where one water molecule condenses on one side of an ice grain while an other molecule sublimates on the other side
450 is equivalent to a situation where the condensing molecule skipped the ice phase, virtually increasing the vapor flux.

We demonstrated that the specific internal boundary conditions governing the sublimation and condensation of water molecules



455 have a significant impact on the macroscopic vapor flux. In particular, we showed that in the case of infinitely fast kinetics the macroscopic flux is enhanced compared to the slow kinetics case, but still cannot exceed the vapor flux that would happen in free air under a similar vapor gradient. This demonstration is confirmed by numerical simulations on both idealized and measured snow microstructures. The discrepancies with previous studies that report vapor fluxes superior to the free air case originate from erroneous computations of how the macroscopic flux was obtained from the microscopic vapor fluxes at the pore scale. We argue that the method used in this article, i.e. volume averaging over an entire microstructure including the ice phase, is the only one consistent with the intuitive expectation of what the vapor flux is for a macroscopic observer. The numerical simulations also indicate that the infinitely fast kinetics and inert ice surface cases respectively are the upper and lower limits for the vapor flux in snow. The use of more complex laws describing the sublimation and condensation of water molecules at the ice surface leads to flux values in between both previously mentioned cases. Moreover, the use of a non-constant attachment coefficient breaks the proportionality between the macroscopic vapor flux and vapor gradient. In that case, it is no longer possible to define a single intrinsic effective diffusion coefficient, independent of the applied macroscopic boundary conditions.

465 *Code availability.* The codes used for the simulations were developed with python3 and ElmerFEM. They will be provided upon request to the corresponding author.

Appendix A: Saturation of vapor in the infinitely fast surface kinetics case

In the case of infinitely fast surface kinetics, and assuming a linear relation between saturation concentration and temperature, the equations governing the vapor concentration are:

$$470 \begin{cases} \operatorname{div}(-D_0 \nabla c) = 0 & (\Omega_a) \\ c = c_{\text{sat}} = AT + B & (\Gamma) \end{cases} \quad (\text{A1})$$

where A and B are two constants characterizing the linear relationship between temperature and vapor concentration, and T is temperature of the ice surface. Thanks to the linearity of the divergence and gradient operators, and owing to the fact that $\nabla B = 0$, the equations can be reformulated to:

$$\begin{cases} \operatorname{div}(\nabla \theta) = 0 & (\Omega_a) \\ \theta = T & (\Gamma) \end{cases} \quad (\text{A2})$$



475 where $\theta = (c - B)/A$ and we have used the fact that D_0 is a non-zero constant to eliminate it from the first equation. Moreover let us recall that in the air temperature T_a is a solution of the following Laplace equation:

$$\begin{cases} \operatorname{div}(\nabla T_a) = 0 & (\Omega_a) \\ T_a = T & (\Gamma) \end{cases} \quad (\text{A3})$$

Systems of Equations A2 and A3 are identical, and since the solution of such a boundary value problem is unique it follows that $T_a = \theta = (c - B)/A$ over the entire pore space. It thus follows that $c = AT_a + B = c_{\text{sat}}(T_a)$ in the pores.

480 **Appendix B: Vapor flux in the Hansen and Folsien, 2015 thermal conductivity**

Hansen and Foslien (2015) proposed that the heat flux q_s through a snow sample under a macroscopic thermal gradient ∇T be expressed as:

$$q_s = (1 - \phi)q_{\text{tub}} + \phi q_{\text{lam}} \quad (\text{B1})$$

485 where q_{tub} and q_{lam} are the heat fluxes through idealized snow structures corresponding respectively to a tubular structure and a lamellae structure, submitted to the same macroscopic thermal gradient ∇T . Concerning the tubular microstructure, one has:

$$q_{\text{tub}} = (1 - \phi)k_i + \phi(k_a + LD_0 \frac{dc_{\text{sat}}}{dT}) \nabla T \quad (\text{B2})$$

where k_i and k_a are the thermal conductivities of ice and air, and L is the latent heat of sublimation of ice. The contribution of the vapor flux is $\phi LD_0 \frac{dc_{\text{sat}}}{dT} \nabla T$, and the vapor flux in the tubular microstructure is $\phi D_0 \frac{dc_{\text{sat}}}{dT} \nabla T = \phi D_0 \nabla C$.

490 Similarly one has concerning the lamellae microstructure:

$$q_{\text{lam}} = \frac{k_i(k_a + LD_0 \frac{dc_{\text{sat}}}{dT})}{(1 - \phi)(k_a + LD_0 \frac{dc_{\text{sat}}}{dT}) + \phi k_i} \nabla T \quad (\text{B3})$$

The contribution of the latent heat flux to q_{lam} is $\frac{\phi k_i LD_0 \frac{dc_{\text{sat}}}{dT}}{(1 - \phi)(k_a + LD_0 \frac{dc_{\text{sat}}}{dT}) + \phi k_i} \nabla T$. Note that the ϕ term in the numerator is omitted in the original Hansen and Foslien (2015) demonstration, leading to an overestimation of latent heat flux. The vapor flux is $\frac{\phi k_i D_0}{(1 - \phi)(k_a + LD_0 \frac{dc_{\text{sat}}}{dT}) + \phi k_i} \nabla C$.

495 Finally, the total vapor flux in the Hansen and Foslien (2015) model is computed as the weighted average of the tubular and lamallae vapor fluxes:

$$F = \left[\phi \frac{\phi k_i D_0}{(1 - \phi)(k_a + LD_0 \frac{dc_{\text{sat}}}{dT}) + \phi k_i} + (1 - \phi) \phi D_0 \right] \nabla C \quad (\text{B4})$$



and the expression in square bracket is therefore the effective vapor diffusion coefficient, that one can show to be inferior to D_0 .

500 *Author contributions.* FD designed research with inputs from PH and KF. FD obtained funding. KF performed research and wrote the paper with inputs from FD and PH.

Competing interests. The authors declare having no competing interests.

Acknowledgements. This work contributes to the APT project (Acceleration of Permafrost Thaw), funded by the Climate Initiative program of the BNP-Paribas Foundation. We thank Jacques Roulle for his help during the tomography scanning and cold-room work. We thank Neige
505 Calonne and Marie Dumont for their valuable inputs on the subject.



References

- Auriault, J.: Heterogeneous medium. Is an equivalent macroscopic description possible?, *Int. J. Engin. Sci.*, 29, 785–795, [https://doi.org/10.1016/0020-7225\(91\)90001-J](https://doi.org/10.1016/0020-7225(91)90001-J), 1991.
- Auriault, J.-L., Boutin, C., and Geindreau, C.: Homogenization of coupled phenomena in heterogenous media, John Wiley & Sons, 2010.
- 510 Calonne, N., Flin, F., Morin, S., Lesaffre, B., du Roscoat, S. R., and Geindreau, C.: Numerical and experimental investigations of the effective thermal conductivity of snow, *Geophys. Res. Lett.*, 38, L23 501, <https://doi.org/10.1029/2011GL049234>, 2011.
- Calonne, N., Geindreau, C., and Flin, F.: Macroscopic modeling for heat and water vapor transfer in dry snow by homogenization, *J. Phys. Chem. B*, 118, 13 393–13 403, <https://doi.org/10.1021/jp5052535>, 2014.
- Christon, M., Burns, P. J., and Sommerfeld, R. A.: Quasi-steady temperature gradient metamorphism in idealized, dry snow, *Numer. Heat*
515 *Transf., Part A: Appl.*, 25, 259–278, <https://doi.org/10.1080/10407789408955948>, 1994.
- Colbeck, S. C.: Theory of metamorphism of dry snow, *J. Geophys. Res. Oceans*, 88, 5475–5482, <https://doi.org/10.1029/JC088iC09p05475>, 1983.
- Colbeck, S. C.: The vapor diffusion coefficient for snow, *Water Resour. Res.*, 29, 109–115, <https://doi.org/10.1029/92WR02301>, 1993.
- Domine, F., Barrere, M., and Sarrazin, D.: Seasonal evolution of the effective thermal conductivity of the snow and the soil in high Arctic
520 herb tundra at Bylot Island, Canada, *Cryosphere*, 10, 2573–2588, <https://doi.org/10.5194/tc-10-2573-2016>, 2016.
- Domine, F., Belke-Brea, M., Sarrazin, D., Arnaud, L., Barrere, M., and Poirier, M.: Soil moisture, wind speed and depth hoar formation in the Arctic snowpack, *J. Glaciol.*, 64, 990–1002, <https://doi.org/10.1017/jog.2018.89>, 2018.
- Fierz, C., Armstrong, R. L., Durand, Y., Etchevers, P., Greene, E., McClung, D. M., Nishimura, K., Satyawali, P. K., and Sokratov, S. A.:
The International Classification for Seasonal Snow on the Ground, 2009.
- 525 Gavriliev, R.: A Model for Calculating the Effective Diffusion Coefficient of Water Vapour in Snow, in: Ninth International Conference on Permafrost, edited by Kane, D. L. and Hinkel, K. M., pp. 505–501, Institute of Northern Engineering, University of Alaska Fairbanks, 2008.
- Giddings, J. C. and LaChapelle, E.: The formation rate of depth hoar, *J. Geophys. Res.*, 67, 2377–2383, <https://doi.org/10.1029/JZ067i006p02377>, 1962.
- 530 Hagenmuller, P., Flin, F., Dumont, M., Tuzet, F., Peinke, I., Lapalus, P., Dufour, A., Roulle, J., Pézard, L., Voisin, D., Ando, E., Rolland du Roscoat, S., and Charrier, P.: Motion of dust particles in dry snow under temperature gradient metamorphism, *Cryosphere*, 13, 2345–2359, <https://doi.org/10.5194/tc-13-2345-2019>, 2019.
- Hansen, A. C. and Foslien, W. E.: A macroscale mixture theory analysis of deposition and sublimation rates during heat and mass transfer in dry snow, *Cryosphere*, 9, 1857–1878, <https://doi.org/10.5194/tc-9-1857-2015>, 2015.
- 535 Lehning, M., Bartelt, P., Brown, B., Fierz, C., and Satyawali, P.: A physical SNOWPACK model for the Swiss avalanche warning: Part II. Snow microstructure, *Cold Reg. Sci. Tech.*, 35, 147–167, [https://doi.org/10.1016/S0165-232X\(02\)00073-3](https://doi.org/10.1016/S0165-232X(02)00073-3), 2002.
- Libbrecht, K. G. and Rickerby, M. E.: Measurements of surface attachment kinetics for faceted ice crystal growth, *J. Cryst. Growth*, 377, 1–8, <https://doi.org/10.1016/j.jcrysgr.2013.04.037>, 2013.
- Malinen, M. and Råback, P.: Elmer Finite Element Solver for Multiphysics and Multiscale Problems, in: *Multiscale Modelling Methods for Applications in Materials Science*, edited by Kondov, I. and Sutmann, G., pp. 101–113, Forschungszentrum Jülich GmbH, 2013.
- 540 Pinzer, B. R., Schneebeli, M., and Kaempfer, T. U.: Vapor flux and recrystallization during dry snow metamorphism under a steady temperature gradient as observed by time-lapse micro-tomography, *Cryosphere*, 6, 1141–1155, <https://doi.org/10.5194/tc-6-1141-2012>, 2012.



- Saito, Y.: Statistical physics of crystal growth, World Scientific, 1996.
- Sokratov, S. A. and Maeno, N.: Effective water vapor diffusion coefficient of snow under a temperature gradient, *Water Resour. Res.*, 36, 1269–1276, <https://doi.org/10.1029/2000WR900014>, 2000.
- Sommerfeld, R. A., Friedman, I., and Nilles, M.: The fractionation of natural isotopes during temperature gradient metamorphism of snow, in: *Seasonal Snowcovers: Physics, Chemistry, Hydrology*, pp. 95–105, Springer, 1987.
- Sturm, M. and Johnson, J. B.: Natural convection in the subarctic snow cover, *J. Geophys. Res. Solid Earth*, 96, 11 657–11 671, <https://doi.org/10.1029/91JB00895>, 1991.
- 545 Torquato, S. and Haslach Jr, H.: Random heterogeneous materials: microstructure and macroscopic properties, *Appl. Mech. Rev.*, 55, B62–B63, 2002.
- Trabant, D. and Benson, C.: Field experiments on the development of depth hoar, *Geol. Soc. Am. Mem.*, 135, 309–322, 1972.
- Vionnet, V., Brun, E., Morin, S., Boone, A., Faroux, S., Le Moigne, P., Martin, E., and Willemet, J.-M.: The detailed snowpack scheme Crocus and its implementation in SURFEX v7.2, *Geosci. Mod. Devel.*, 5, 773–791, <https://doi.org/10.5194/gmd-5-773-2012>, 2012.
- 555 Yosida, Z., Oura, H., Kuroiwa, D., Huzioka, T., Kojima, k., Aoki, S.-I., and Kinoshita, S.: Physical Studies on Deposited Snow. I. Thermal Properties., *Contributions from the Institute of Low Temperature Science*, 7, 19–74, 1955.